Self-Assembled Monolayers of CH 3 COS–Terminated Surfactant-Encapsulated Polyoxometalate Complexes

ARTICLE *in* LANGMUIR · JUNE 2008

Impact Factor: 4.46 · DOI: 10.1021/la702335r · Source: PubMed

Self-Assembled Monolayers of CH_3COS^- Terminated Surfactant-Encapsulated Polyoxometalate Complexes

Hang Sun,[†] Weifeng Bu,[†] Yancai Li,[‡] Haolong Li,[†] Lixin Wu,*[,†] Changqing Sun,[‡] Bin Dong,[†,§] Ruifen Dou,[§] Lifeng Chi,[†,§] and Andreas Schaefer[||]

State Key Laboratory of Supramolecular Structure and Materials and College of Chemistry, Jilin University, Changchun 130012, People's Republic of China, and Physikalisches Institut and Center for Nanotechnology (CeNTech), Westfälische Wilhelms-Universität, 48149 Münster, Germany, and NanoAnalytics GmbH, 48149 Münster, Germany

Received August 9, 2007. In Final Form: October 15, 2007

Self-assembled monolayers (SAMs) on gold surfaces based on three kinds of acetylthio−surfactant-encapsulated polyoxometalate clusters (thio-SECs) terminated with multiple CH_3COS^- groups, $(NC_{26}H_{55}S(CO)CH_3)_6H_2[Co(H_2O)CoW_{11}O_{39}]$, $(NC_{26}H_{55}S(CO)CH_3)_{13}H_3[Co_4(H_2O)_2(P_2W_{15}O_{56})_2]$, and $(NC_{26}H_{55}S(CO)CH_3)_{13}[Fe_4(H_2O)_2(P_2W_{15}O_{56})_2]Br$, have been prepared, which is representative of a general methodology to fabricate polyoxometalate-based SAMs. Thio-SECs self-assembled into monolayers on gold surfaces through the hydrolysis of CH_3COS^- groups and the subsequent formation of S−Au bonds, which was confirmed by grazing angle infrared spectroscopy, X-ray photoelectron spectroscopy, and ellipsometric and scanning tunneling microscopy (STM) measurements. Furthermore, the SAMs of the thio-SECs possess closely packed structures, and the local short-range order is clearly observed in the magnified STM image. We have also investigated the electrochemical behavior of SAMs of thio-SECs by cyclic voltammetry in detail, and the redox potential of the original polyoxometalates has been well retained. The electrochemical signals of the SAMs are very weak because of the small moiety of thio-SECs that are electrochemically accessible in the cyclic voltammetry experiments. The polyoxometalate-modified electrodes that we prepared are not only highly ordered in the local short range but also stable in electrochemical cycling because of the multiple S−Au bonds of thio-SECs on the gold substrates that aid in the construction of functional materials such as electrochemical and electrocatalytic devices.

Introduction

Polyoxometalates (POMs) are a large class of inorganic compounds composed of the early transition elements, especially vanadium, molybdenum, and tungsten, and have extensive applications in diverse fields such as catalysis, medicine, and material science because of their topological and electronic versatility.[1] One of the most important electronic properties of these metal oxide clusters is that they are able to accept one or several electrons, forming so-called heteropolyblue. The blue electrons undergo a rapid intramolecular electron transfer (such as $\sim 10^{11}$ to 10^{12} s^{-1} in a $[PW_{12}O_{40}]^{4-}$ cluster) via a thermal hopping mechanism.[2] The reduction process of POMs is reversible and occurs with marginal structural rearrangement. The electrochemical properties of POMs have attracted increasing attention for their practical applications in areas such as catalysis and electrocatalysis, molecular material, and corrosion inhibition.[3] Of particular relevance is the immobilization of POMs onto surfaces to incorporate the functionality available with POMs into a heterogeneous catalytic environment. At present, there are three methods commonly used to immobilize POMs onto the electrode surface.[3a] The first is the adsorption of POMs onto the electrode surface by dip coating, the second is to entrap POMs in polymers on the electrode surface, and the third is the electrodeposition of POMs onto the electrode surface within the POMs solution under constant potential. Furthermore, electrodes of hybrid organic-POM multilayered structures have been produced by the LB technique and electrostatic layer-by-layer assembly with cationic polyelectrolytes.[4] In particular, the preparation of highly ordered self-assembled monolayers (SAMs) of POMs at conducting substrates, for instance, gold and silver, is still a challenge because monolayers have many desirable features that aid in the construction of functional materials in performing basic electronic functions of POMs, such as electrochemical and electrocatalytic devices. It is well known that highly ordered monolayers of POMs can be obtained by self-assembling the clusters directly onto solid supports such as graphite, silver, and gold.[5] However, only a SAM of α-$H_4SiW_{12}O_{40}$ on a silver substrate is stable because of a strong covalent interaction between POM and the silver substrate.[5b,5c] Therefore, a general methodology that could be extensively applied in a POM system with convenience is indispensable to the fabrication of stable SAMs of POMs at the conducting substrates.

In the past 20 years, self-assembled monolayer chemistry has provided a facile and versatile route to the functionalization of

* To whom correspondence should be addressed. E-mail: wulx@jlu.edu.cn.

† State Key Laboratory for Supramolecular Structure and Materials and College of Chemistry, Jilin University.

‡ College of Chemistry, Jilin University.

§ Westfälische Wilhelms-Universität.

|| NanoAnalytics GmbH.

(1) (a) Pope, M. T.; Müller, A. *Angew. Chem., Int. Ed.* **1991**, *30*, 34. (b) *Chem. Rev.* **1998**, *98*, 1. The entire issue is devoted to polyoxometalates. (c) Pope, M. T.; Müller, A. *Polyoxometalate Chemistry from Topology via Self-Assembly to Application*; Kluwer Academic Publishers: Dordrecht, The Netherlands, 2001. (d) Casañ-Pastor, N.; Gómez-Romero, P. *Front. Biosci.* **2004**, *9*, 1759.

(2) (a) Sanchez, C.; Livage, J.; Launay, J. P.; Fournier, M. *J. Am. Chem. Soc.* **1983**, *105*, 6817. (b) Weinstock, I. A. *Chem. Rev.* **1998**, *98*, 113.

(3) (a) Coronado, E.; Gómez-García, C. J. *Chem. Rev.* **1998**, *98*, 273. (b) Kulesza, P. J.; Faulkner, L. R.; Chen, J.; Klemperer, W. G. *J. Am. Chem. Soc.* **1991**, *113*, 379. (c) Keita, B.; Abdeljalil, E.; Nadjo, L.; Contant, R.; Belghiche, R. *Langmuir* **2006**, *22*, 10416. (d) Kuhn, A.; Anson, F. C. *Langmuir* **1996**, *12*, 5481.

(4) (a) Clemente-León, M.; Coronado, E.; Gómez-García, C. J.; Mingotaud, C.; Ravaine, S.; Romualdo-Torres, G.; Delhaès, P. *Chem.—Eur. J.* **2005**, *11*, 3979. (b) Liu, S.; Kurth, D. G.; Möhwald, H.; Volkmer, D. *Adv. Mater.* **2002**, *14*, 225. (c) Liu, S.; Kurth, D. G.; Bredenkötter, B.; Volkmer, D. *J. Am. Chem. Soc.* **2002**, *124*, 12279.

10.1021/la702335r CCC: $40.75
Published on Web 03/25/2008

solid surfaces; that is, immersion in a solution of organic molecular absorbates leads to ordered arrays of these building blocks on the substrates with or without chemical bindings.[6] This technique provides the possibility for us to organize POMs on solid surfaces because almost all POMs can be easily included without structure and function impairment by using a water-insoluble shell composed of organic molecules based on cooperatively electrostatic interactions. Most surfactant-encapsulated clusters are very soluble in organic media such as chloroform, benzene, and toluene and are readily processed into thin films by spin coating, simple casting, and the LB technique.[7,8] In addition, by replacing the hydrophobic terminals with functional groups, we have chemically embedded the complexes into polymer and silica dioxide sol−gel matrices in a controllable way.[9] On the basis of this strategy, recent progress in POM chemistry offers a good opportunity to build up SAMs containing POMs on the surface of solid substrates.

In this article, we have prepared three different acetylthio (CH_3COS-) group-terminated surfactant-encapsulated polyoxometalate clusters (thio-SECs) and have studied their SAMs on gold surface. The structure of the prepared SAMs was characterized in detail by grazing angle infrared spectroscopy, X-ray photoelectron spectroscopy (XPS), ellipsometry, and scanning tunneling microscopy (STM). Furthermore, the electrochemical behavior of the SAMs has been investigated by cyclic voltammetry.

Experimental Section

Materials. POMs ($K_8[Co(H_2O)CoW_{11}O_{39}]$ (POM-1), $Na_{16}[Co_4(H_2O)_2(P_2W_{15}O_{56})_2]$ (POM-2) and $Na_{12}[Fe_4(H_2O)_2(P_2W_{15}O_{56})_2]$ (POM-3)) were freshly prepared according to literature procedures.[10] 1,12-Dibromododecyl and *N*,*N*-dimethyldodecylamine were purchased from Fluka and Acros Organics, respectively, and used as received. Gold-coated solid substrates were prepared by vapor deposition in vacuum on mica that precoated a layer of chromium to enhance the binding strength of gold film, and both were evaporated at a pressure of $5-10^{-6}$ mbar from a resistively heated tungsten boat. The prepared gold-coated slides were then flame annealed to make the gold slide of the (111) surface up to even micrometer-sized flat areas.[11]

Synthesis of the CH_3COS-Terminated Surfactant. The synthesis of dodecyl(12-acetylthio)dimethylammonium bromide (S-1) was completed from the esterification of 1,12-dibromododecyl with potassium ethanethioate and subsequent quarternization with *N*,*N*-dimethyldodecylamine.[12] A mixture of 1,12-dibromododecyl (8 g, 24.38 mmol) and potassium ethanethioate (0.7 g, 6.13 mmol) in 100 mL of acetonitrile was stirred for 24 h under reflux. The solvent was evaporated, and the residue was treated with chloroform and filtered. The organic phase was washed with water, dried over anhydrous Na_2SO_4, and filtered. After the evaporation of solvent, the residue was further purified to obtain acetylthio 12-bromododecyl ester by column chromatography on silica gel using 97/3.5 (v/v) cyclohexane/ethyl acetate as an eluent (yield 66.7%). Then a mixture of the obtained acetylthio 12-bromododecyl ester (0.2 g, 0.94 mmol) and *N*,*N*-dimethyldodecylamine (0.4 g, 1.24 mmol) in 100 mL of acetonitrile was stirred for 24 h under reflux. After cooling to room temperature, the mixture was concentrated to 3−5 mL under reduced pressure and to the residue was added 30 mL of cold diethyl ether dropwise. Then, the mixture was stored at 0 °C for 3 days. The formed white precipitates were filtered and washed with cold diethyl ether to give the final surfactant, S-1 (yield 82%). For S-1, FTIR (KBr, cm^{-1}): 2956, 2919, 2848, 1690, 1494, 1468, 1402, 1381, 1353, 1147, 1112, 967, 871, 760, 721, 636, 528. ^1H NMR ($CDCl_3$, 500 MHz) δ: 0.88 (t, $J = 7.5$ Hz, 3H, CH_3), 1.33 (m, 26H, CH_2), 1.39 (m, 8H, CH_2), 1.55 (m, $J = 7.5$ Hz, 2H, CH_2), 1.68 (m, $J = 7.5$ Hz, 4H, CH_2), 2.34 (s, 3H, CH_3COS-), 2.86 (t, $J = 7.5$ Hz, 2H, SCH_2), 3.41 (s, 6H, NCH_3),3.52 (t, $J = 7.5$ Hz, 4H, NCH_2). Anal. Calcd. for S-1 ($C_{28}H_{58}NOSBr\cdot H_2O$, 554.75): C 60.62, H 10.90, N 2.52. Found: C 61.09, H 10.90, N 2.56.

Preparation of Thio-SECs. We have encapsulated the three POMs with S-1, forming thio-SECs that are terminated with the same number of CH_3COS- groups as that of surfactant cations on the surface of POMs, and can form the SAMs on metal surfaces such as gold and silver. These thio-SECs were synthesized according to the previously reported procedures,[8] as exemplified by SEC-1. POM-1 was dissolved in aqueous solution, and then a chloroform solution of S-1 was added with stirring. The initial molar ratio of S-1 to POM-1 was controlled at 6.5:1. The organic phase was separated, and $(S\text{-}1)_6H_2[Co(H_2O)CoW_{11}O_{39}]$ (SEC-1) was obtained by evaporating the chloroform to dryness. Then, the sample was further dried under vacuum until its weight remained constant. Following a similar procedures, $(S\text{-}1)_{13}H_3[Co_4(H_2O)_2(P_2W_{15}O_{56})_2]$ (SEC-2) and $(S\text{-}1)_{13}[Fe_4(H_2O)_2(P_2W_{15}O_{56})_2]Br$ (SEC-3) were prepared. Coordination polyhedral representations of the POMs used for encapsulation, with a chemical formula of S-1 and a schematic drawing of the complexes, are shown in Figure 1. For SEC-1, FTIR (KBr, cm^{-1}): 2956, 2924, 2852, 1695, 1484, 1465, 1402, 1379, 1352, 1134, 1110, 925, 868, 754, 723, 626, 454. Anal. Calcd. for SEC-1 ($C_{168}H_{352}N_6O_{46}S_6Co_2W_{11}$, 5525.2): C 36.52, H 6.42, N 1.23. Found: C 37.40, H 6.71, N 1.52. For SEC-2, FTIR (KBr, cm^{-1}): 2956, 2924, 2852, 1696, 1482, 1465, 1400, 1380, 1353, 1134, 1087, 1051, 942, 908, 820, 770, 723, 626, 525. Anal. Calcd. for SEC-2 ($C_{364}H_{761}N_{13}S_{13}P_4Co_4W_{30}O_{127}$, 13 644): C 32.04, H 5.62, N 1.33. Found: C 32.02, H 5.64, N 1.17. For SEC-3, FTIR (KBr, cm^{-1}): 2956, 2924, 2852, 1696, 1482, 1465, 1400, 1379, 1356, 1135, 1088, 1053, 947, 911, 820, 733, 721, 625, 522. Anal. Calcd. for SEC-3 ($C_{364}H_{758}N_{13}S_{13}P_4Fe_4W_{30}O_{127}Br$, 13709): C 31.89, H 5.57, N 1.33. Found: C 31.95, H 5.58, N 1.14.

Preparation of Thio-SECs SAMs. The SAMs of SEC-1, SEC-2, and SEC-3 were prepared as follows. About 50 μL of aqueous NH_4OH (30%) was added to 5 mL of THF solutions of SEC-1, SEC-2, and SEC-3 (3 mg/mL) for deacylation, and the pH of the

(5) (a) Klemperer, W. G.; Wall, C. G. *Chem. Rev.* **1998**, *98*, 297. (b) Ge, M.; Zhong, B.; Klemperer, W. G.; Gewirth, A. A. *J. Am. Chem. Soc.* **1996**, *118*, 5812. (c) Lee, L.; Wang, J. X.; Adžić, R. R.; Robinson, I. K.; Gewirth, A. A. *J. Am. Chem. Soc.* **2001**, *123*, 8838. (d) Barteau, M. A.; Lyons, J. E.; Song, I. K. *J. Catal.* **2003**, *216*, 236. (e) Song, I. K.; Shnitser, R. B.; Cowan, J. J.; Hill, C. L.; Barteau, M. A. *Inorg. Chem.* **2002**, *41*, 1292. (f) Song, I. K.; Barteau, M. A. *Kor. J. Chem. Eng.* **2002**, *19*, 567. (g) Song, I. K.; Lyons, J. E.; Barteau, M. A. *Catal. Today* **2003**, *81*, 137. (h) Kaba, M. S.; Song, I. K.; Duncan, D. C.; Hill, C. L.; Barteau, M. A. *Inorg. Chem.* **1998**, *37*, 398. (i) Song, I. K.; Kaba, M. S.; Barteau, M. A. *Langmuir* **2002**, *18*, 2358. (j) Kaba, M. S.; Song, I. K.; Barteau, M. A. *J. Phys. Chem. B* **2002**, *106*, 2337. (k) Alam, M. S.; Dremov, V.; Müller, P.; Postnikov, A. V.; Mal, S. S.; Hussain, F.; Kortz, U. *Inorg. Chem.* **2006**, *45*, 2866. (l) Errington, R. J.; Petkar, S. S.; Horrocks, B. R.; Houlton, A.; Lie, L. H.; Patole, S. N. *Angew. Chem., Int. Ed.* **2005**, *44*, 1254.

(6) (a) Ulman, A. *Chem. Rev.* **1996**, *96*, 1533. (b) Love, J. C.; Estroff, L. A.; Kriebel, J. K.; Nuzzo, R. G.; Whitesides, G. M. *Chem. Rev.* **2005**, *105*, 1103.

(7) (a) Kurth, D. G.; Lehmann, P.; Volkmer, D.; Cölfen, H.; Koop, M. J.; Müller, A.; Du, Chesne, A. *Chem.—Eur. J.* **2000**, *6*, 385. (b) Volkmer, D.; Du Chesne, A.; Kurth, D. G.; Schnablegger, H.; Lehmann, P.; Koop, M. J.; Müller, A. *J. Am. Chem. Soc.* **2000**, *122*, 1995. (c) Kurth, D. G.; Lehmann, P.; Volkmer, D.; Müller, A.; Schwahn, D. *J. Chem. Soc., Dalton Trans.* **2000**, 3989. (d) Polarz, S.; Smarsly, B.; Antonietti, M. *Chem. Phys. Chem.* **2001**, *2*, 457. (e) Volkmer, D.; Bredenkötter, B.; Tellenbröker, J.; Kögerler, P.; Kurth, D. G.; Lehmann, P.; Schnablegger, H.; Schwahn, D.; Piepenbrink, M.; Krebs, B. *J. Am. Chem. Soc.* **2002**, *124*, 10489.

(8) (a) Bu, W.; Wu, L.; Hou, X.; Fan, H.; Hu, C.; Zhang, X. *J. Colloid Interface Sci.* **2002**, *251*, 120. (b) Bu, W.; Fan, H.; Wu, L.; Hou, X.; Hu, C.; Zhang, G.; Zhang, X. *Langmuir* **2002**, *18*, 6398. (c) Bu, W.; Zhang, J.; Wu, L.; Tang, A.-C. *Chin. J. Chem.* **2002**, *20*, 1514. (d) Bu, W.; Wu, L.; Zhang, X.; Tang, A.-C. *J. Phys. Chem. B* **2003**, *107*, 13425. (e) Bu, W.; Wu, L.; Tang, A.-C. *J. Colloid Interface Sci.* **2004**, *269*, 472. (f) Bu, W.; Li, W.; Li, H.; Wu, L.; Tang, A.-C. *J. Colloid Interface Sci.* **2004**, *274*, 200. (g) Bu, W.; Li, H.; Li, W.; Wu, L.; Zhai, C.; Wu, Y. *J. Phys. Chem. B* **2004**, *108*, 12776. (h) Bu, W.; Li, H.; Sun, H.; Yin, S.; Wu, L. *J. Am. Chem. Soc.* **2005**, *127*, 8016.

(9) (a) Li, H.; Qi, W.; Li, W.; Sun, H.; Bu, W.; Wu, L. *Adv. Mater.* **2005**, *17*, 2688. (b) Qi, W.; Li, H. *Adv. Mater.* **2007**, *19*, 1983.

(10) (a) Baker, L. C. W.; McCutcheon, T. P. *J. Am. Chem. Soc.* **1956**, *78*, 4503. (b) Finke, R. G.; Droege, M. W.; Domaille, P. J. *Inorg. Chem.* **1987**, *26*, 3886. (c) Zhang, X.; Chen, Q.; Duncan, D. C.; Campana, C. F.; Hill, C. L. *Inorg. Chem.* **1997**, *36*, 4208.

(11) (a) Schäfer, A. H.; Seidel, C.; Chi, L.; Fuchs, H. *Adv. Mater.* **1998**, *10*, 839. (b) Bucher, J. P.; Santesson, L.; Kern, K. *Langmuir* **1994**, *10*, 979.

(12) Yokokawa, S.; Tamada, K.; Ito, E.; Hara, M. *J. Phys. Chem. B* **2003**, *107*, 3544.

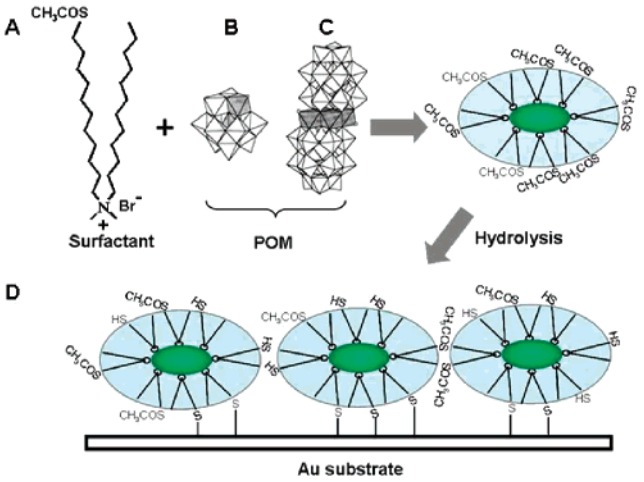

Figure 1. Molecular structure of S-1 (A), coordination polyhedral representation of POM-1 (B), POM-2 and POM-3 (C) clusters in this study, and schematic representation of POM-based SAMs (D).

obtained mixed solutions is about 8.5, under which condition the structure of the encapsulated POMs could not be affected. Then, the Au-coated substrates were immersed in the above obtained mixed solutions for 24 h, respectively, rinsed thoroughly with THF, and dried in a stream of nitrogen.

Measurements. Fourier transform infrared (FTIR) spectral measurements were performed on a Bruker IFS66V FTIR spectrometer equipped with a DGTS detector for thio-SEC solids (32 scans) and with an MCT detector for SAMs of thio-SECs (1024 scans). The spectra were recorded with a resolution of 4 cm^{-1}. The reflection−absorption IR spectrum was measured at an angle of incidence of 80° and a polarized angle of 90°. ^1H NMR spectra (TMS) were recorded on a Bruker UltraShield 500 MHz spectrometer. The surface pressure−area (π−A) isotherms of thio-SECs were carried out on a Nima 622D Langmuir trough (double troughs) with a Wilhelmy plate balance at a constant barrier rate of 20 cm^2/min. The element analysis was measured on a Flash EA1112 analyzer from ThermoQuest Italia S.P.A. Electrochemical experiments were performed with a CHI 660A electrochemical analyzer (CH Instruments). The XPS analysis was done using an ESCALAB 250 from Thermo VG Scientific in which monochromatic Al Kα X-rays were used (15 kV, 150 W, ~500 μm spot diameter). Quantitative information about the surface composition was calculated from survey spectra using the standard Scofield sensitivity factors.[13] The complete error can be estimated to be about 10% typically. The casting films of thio-SECs were characterized by wide-angle X-ray diffraction (XRD), which were carried out on a Rigaku X-ray diffractometer (D/max rA using Cu Kα radiation at a wavelength of 1.542 Å). Ellipsometric measurements were carried out with a I-Elli2000 ellipsometer from NFT Co., Germany, at an angle of incidence of $\Phi = 60°$ and a laser source with a wavelength of $\lambda = 532$ nm. STM investigation was performed using a commercial Nanoscope III scanning tunneling microscope (Digital Instrument Co., Santa Barbara, CA) with mechanically cut Pt/Ir (90/10) tips at ambient temperature.

Results and Discussion

Structural Characterization of Thio-SEC SAMs. The SAMs of thio-SECs were characterized through grazing angle reflection−absorption IR spectroscopy, and the detail assignments were summarized in Table 1. Here, we have analyzed the IR spectra in detail by taking SEC-3 as an example (Figure 2). The CH_2 antisymmetric and symmetric stretching bands of the SAM of SEC-3 appear at 2927 and 2854 cm^{-1}, respectively, corresponding to the disordered alkyl chains of surfactant on POM-3.

(13) Scofield, J. H. *J. Electron Spectrosc. Relat. Phenom.* **1976**, *8*, 129.

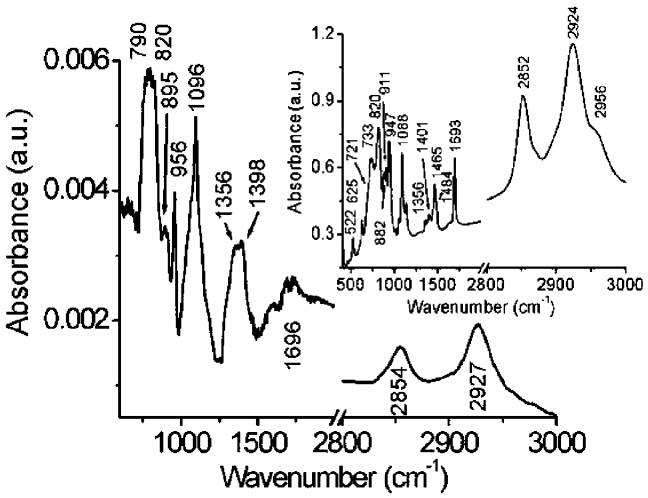

Figure 2. Reflection−absorption IR spectrum of SEC-3 SAM on a gold plate. (Inset) FTIR absorption spectrum of SEC-3 in the solid state in a KBr pellet.

Table 1. Assignments of Infrared Spectra of SEC-1, SEC-2, and SEC-3 in the Solid State and at the SAMs

SEC-1		SEC-2		SEC-3		
solid	SAM	solid	SAM	solid	SAM	assignments
2956		2956		2956		CH_3 antisym. str.
2924	2928	2924	2927	2924	2927	CH_2 antisym. str.
2852	2855	2852	2854	2852	2854	CH_2 sym. str.
1695	1694	1696	1696	1696	1693	C═O stretch
1484		1482		1484		CH_2N scissoring
1465		1465		1465		CH_2 scissoring
1402	1401	1400	1400	1400	1400	CH_2−S scissoring
1379	1380	1380	1380	1379	1379	CH_3 scissoring
1352	1352	1353	1352	1356	1356	CH_2−S scissoring
		1087	1091	1088	1096	P−O antisym. str.
925	926	942	935	947	956	$W-O_d$ antisym. str.
868	875	908	860	911	895	$W-O_b-W$ antisym. str.
758	744	820	800	820	820	$W-O_c-W$ antisym. str.
		770	733	733	790	$W-O_c-W$ antisym. str.
723		723		721		CH_2 rocking

The W−O antisymmetric vibrational modes of POM-3 are clearly observed at 956, 895, 820, and 790 cm^{-1}. The band at 1096 cm^{-1} can be attributed to P−O antisymmetric stretching mode. The relative intensity of the band at 1696 cm^{-1} that is assigned to the vibration of carboxyl in the SAMs becomes much lower than that in the solid of thio-SECs, indicative of the partial hydrolysis of CH_3COS- groups.

XPS measurements reveal the presence of POMs in the SAMs on the basis of the intensities of the binding energy of tungsten and oxygen atoms (Figure 3A). Furthermore, the binding energy of $S_{2p3/2}$ electrons can be used not only to prove the existence of sulfur atoms but also to discriminate between free (163.4 eV) and Au-bound (161.9 eV) sulfur atoms in the SAMs of thiol molecules, and their ratios could be estimated from their fitted peak areas.[14] The broad bands of SEC-3 SAM from 161 to 165 eV are fit using two S_{2p} doublets with 2:1 area ratios and a splitting of 1.2 eV (Figure 3B). The two binding energies appearing at 161.80 and 163.70 eV for $S_{2p3/2}$ just correspond to Au-bound and surface-unbound sulfur atoms in the SAM, respectively. The ratio between surface-unbound and surface-bound sulfur atoms is estimated to be 1:3 on the basis of their fitted peak areas. Such a large fraction of Au-unbound sulfur

(14) (a) Li, Y.; Huang, J.; McIver, R. T., Jr.; Hemminger, J. C. *J. Am. Chem. Soc.* **1992**, *114*, 2428. (b) Schoenfisch, M. H.; Pemberton, J. E. *J. Am. Chem. Soc.* **1998**, *120*, 4502. (c) Rieley, H.; Kendall, G. K.; Zemicael, F. W.; Smith, T. L.; Yang, S. *Langmuir* **1998**, *14*, 5147.

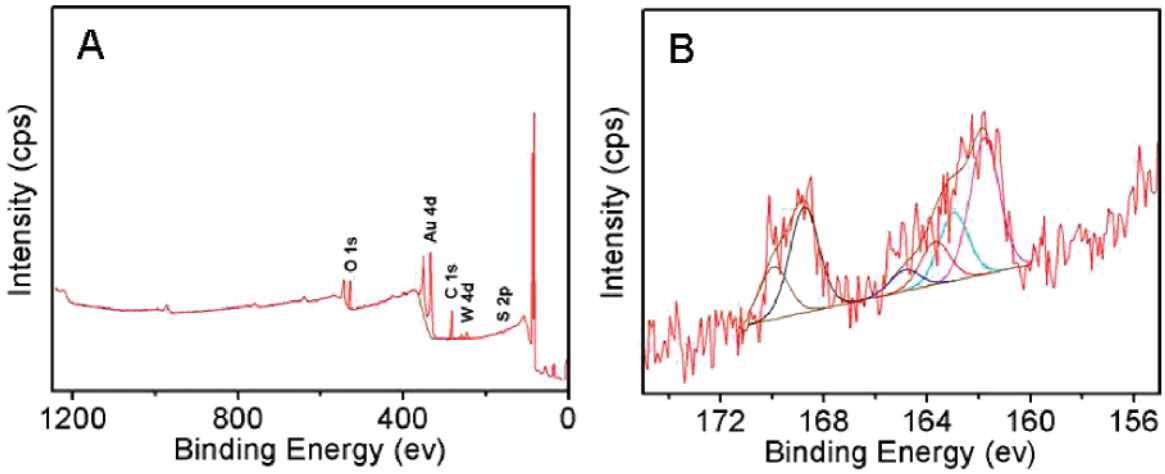

Figure 3. (A) XPS spectrum of the SAM of SEC-3 on a gold substrate and (B) its fittings in the magnified signal of S_{2p}.

Table 2. Peak Positions, Ascriptions, and % Fitted Peak Areas of XPS Signals of the SAMs of SEC-1, SEC-2, and SEC-3 on Gold Substrates Together with Calculated Unbound-S/Bound-S Ratios

SAMs	peak position	ascription	% fitted peak area	unbound-S/ bound-S ratios
	161.80	R−S−Au(1)	36.2	2/3
	162.98	R−S−Au S(1)	18.1	
SEC-1	163.70	−SH/S−S(1)	23.0	
	164.88	−SH/S−S(2)	11.5	
	168.32	sulfate/sulfone(1)	7.4	
	169.50	sulfate/sulfone(2)	3.7	
	161.80	R−S−Au (1)	27.2	2/3
	162.98	R−S−Au S(1)	13.6	
SEC-2	163.70	−SH/S−S(1)	17.0	
	164.88	−SH/S−S(2)	8.5	
	169.51	sulfate/sulfone(1)	22.5	
	170.69	sulfate/sulfone(2)	11.3	
	161.80	R−S−Au (1)	31.9	1/3
	162.98	R−S−Au S(1)	15.9	
SEC-3	163.70	−SH/S−S(1)	10.1	
	164.88	−SH/S−S(2)	5.0	
	168.77	sulfate/sulfone(1)	24.7	
	169.95	sulfate/sulfone(2)	12.3	

atoms is not surprising considering the core−shell structure of the thio-SECs, as schematically presented in Figure 1. Similarly, the peak at about 169 eV is fit using one S_{2p} doublet with a 2:1 area ratio and a splitting of 1.2 eV, which corresponds to a binding energy of 168.77 eV for $S_{2p3/2}$. This high-energy sulfur signal can be attributed to the characteristics of highly oxidized sulfur atoms (+6 state, such as sulfonic acid) because of the molecular oxygenation of atmospheric contamination physisorbed onto the films.[14] In our case, it is also possible that POMs activate the molecular oxygen as a catalyst for sulfur oxidation.[15] Other SEC SAMs present very similar spectra to those of SEC-3, and the detail peak positions, ascriptions, fitted peak areas of XPS signals of the SAMs of SEC-1, SEC-2, and SEC-3 on gold substrates together with calculated unbound-S/bound-S ratios are summarized in Table 2.

Ellipsometric measurements reveal that the thickness of the SAMs of SEC-1, SEC-2, and SEC-3 are 3.2, 3.5, and 3.4 nm, respectively. According to the Langmuir isotherms of SEC-1, SEC-2, and SEC-3, the limiting molecular areas are determined to be 6.16, 11.82, and 9.78 nm^2, respectively, by extending the condensed phase to zero pressure (Figure 4). Because the alkyl

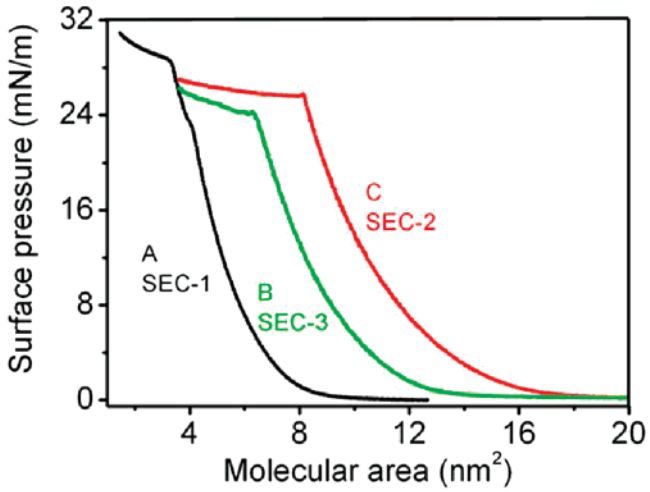

Figure 4. Langmuir isotherms of SEC-1 (A), SEC-3 (B), and SEC-2 (C).

chains of the surfactants on the POM surface are distorted, they can be treated as a flexible shell around the core. Thus, these occupied areas on solid substrates are related to the closest distance between thio-SECs. Considering thio-SECs to be spherically shaped objects, the average diameters of SEC-1, SEC-2, and SEC-3 are estimated to be 2.8, 3.9, and 3.5 nm, respectively. The XRD measurement indicates that the solvent-casting films of SEC-1, SEC-2, and SEC-3 possess lamellar structures with spacings of 2.8, 3.0, and 2.9 nm, respectively, corresponding to single layers of thio-SECs (Figure 5). POM-1 is round, and POM-2 and POM-3 are elliptical. POM-2 and POM-3 should be parallel with the long axis of the substrate because there are more CH_3-COS-terminated surfactants distributed in the long axis than in the short axis. Combining the diameter of POM-1 (1.04 nm) and the alkyl chain length of the CH_3CO- terminated surfactant that is assumed to be fully extended (1.67 nm), the total thickness of a single layer of SEC-1 could be estimated to be 4.4 nm. Similarly, the calculated diameters of SEC-2 and SEC-3 in their short axes are both about 4.3 nm. These XRD data, Langmuir monolayer estimations, and ellipsometric results correspond well to the calculated diameters of the SECs. Therefore, we believe that SEC-1, SEC-2, and SEC-3 form self-assembled monolayers on gold substrates. Furthermore, we have tried other concentrations of SECs for self-assembly and have found that the monolayer structure could remain in a wide range of solution concentration from 0.5 to 10 mg/mL.

(15) Okun, N. M.; Anderson, T. M.; Hill, C. L. *J. Am. Chem. Soc.* **2003**, *125*, 3194.

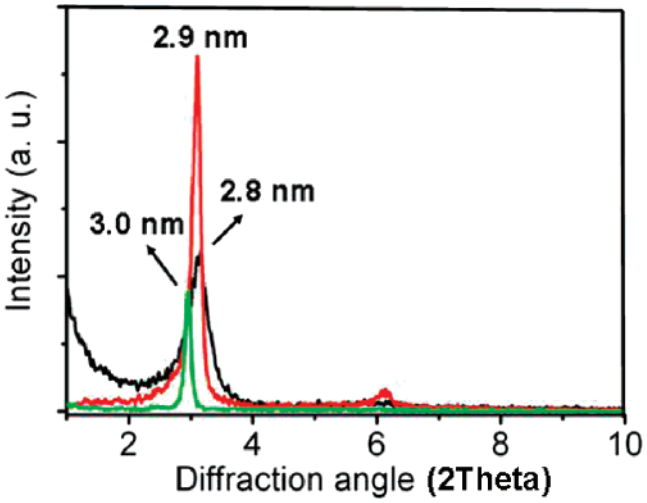

Figure 5. XRD patterns of SEC-1 (2.8 nm), SEC-2 (3.0 nm), and SEC-3 (2.9 nm) solvent-casting films in the low-angle region.

From the results of short-time immersion, we can observe the absorption of SEC complexes on gold surfaces. The STM image of the SAM of SEC-3, after about 10 min of immersion, shows well-isolated clusters with a diameter of 3 to 4 nm (Figure 6A), and the cluster size corresponds well to the Langmuir results. When the immersion time increases to 24 h, the STM image exhibits some defects (i.e., randomly distributed holes in a diameter range of 5 to 10 nm), which is frequently observed in the SAMs of alkanethiols (Figure 6B).[11a] The depth of the holes is approximately 0.3 nm, which is much lower than the average diameter (3.5 nm) of SEC-3, and thus the surface is fully covered. The holes in the present case may result from the disordered alkyl chains of thio-SECs on the gold substrate, which is supported by their IR spectra. However, local short-range order is clearly observed in the magnified STM image of the SAM of SEC-3 (Figure 6C), and the cluster size is also consistent with the value deduced from Langmuir monolayers. Similar results are also observed in the SAMs of SEC-1 and SEC-2. Therefore, we suggest that the SAMs of SEC-1, SEC-2, and SEC-3 possess closely packed structures. Further evidence comes from a penetration study of $[Fe(CN)_3]^{3-}/[Fe(CN)_3]^{4-}$ (1 mM) in aqueous solutions.

Electrochemistry of Thio-SEC SAMs. The cyclic voltammetry of $[Fe(CN)_3]^{3-}/[Fe(CN)_3]^{4-}$ at a freshly polished gold electrode offers a reversible wave at $E_{1/2} = 0.184$ V vs Ag/AgCl (Figure 7A, line a). The intensity of the reversible wave decreases for the gold electrode after about 10 min of immersion in solutions of SEC-1, SEC-2, and SEC-3 (Figure 7A, line b), and almost no detectable electrochemical response associated with the $[Fe(CN)_3]^{3-}/[Fe(CN)_3]^{4-}$ redox couple was observed for gold electrodes modified with the SAMs of SEC-1, SEC-2, and SEC-3 (immersion for 24 h), respectively, in the same solution of $[Fe(CN)_3]^{3-}/[Fe(CN)_3]^{4-}$ (Figure 7A, line c). Therefore, these SAMs must be densely covered and exhibit an impenetrable barrier, which is consistent with th STM results. The cyclic voltammetry for a SAM of SEC-1 on a freshly polished gold electrode in a 0.2 M Na_2SO_4 + 0.05 M H_2SO_4 aqueous solution exhibits two two-electron reduction/oxidation waves at $E_{1/2} = -0.293$ and -0.443 V, which are ascribed to the W^{VI}/W^{V} redox reactions (Table 3). Two similar two-electron reduction/oxidation waves of a SAM of SEC-2 appear at $E_{1/2} = -0.289$ and -0.464 V (Figure 7B). In contrast, the SAM of SEC-3 offers two-electron Fe-centered waves at $E_{1/2} = -0.098$ V besides a couple of two-electron W^{VI}/W^{V} redox waves at $E_{1/2} = -0.300$ and -0.385 V. The cathodic current that appeared at more negative potentials is attributed to the reduction of residual oxygen existed in the cells. Here, the SAM-modified electrode shows the catalytic reduction of residual oxygen, and the cathodic catalytic current decreases upon degassing the solution with nitrogen as seen in the Supporting Information. The electrochemical signals of the SAMs of thio-SECs are very weak; for example, the reduction wave of SEC-2 at -0.273 V offers a current of only 0.233 μA, which is comparable to that of the residual oxygen in the water of the cells although the cells have been degassed for about 3 h with nitrogen. Therefore, we cannot detect their electrochemical signals at the more negative potentials for W^{VI}/W^{V} redox waves and the more positive potentials for the Fe-centered waves, which are shown in the cyclic voltammograms of the aqueous solutions of POM-1,[16a] POM-2,[16b] and POM-3.[16b] It should be noted that the redox signals of the SAMs of thio-SECs are shifted to more negative or positive potentials compared with those of corresponding POMs,[16] which are attributed to the strong inductive effect caused by the cationic surfactants. The surface coverage of redox-active adsorbate monolayer films is usually determined by the integration of redox waves associated with surface-confined species.[17,18] The surface coverage of the SAMs of SEC-1, SEC-2, and SEC-3 can be calculated to be 1.1×10^{-12}, 1.8×10^{-12}, and 1.5×10^{-12} mol/cm^2, respectively, corresponding to average areas of 150.9, 246.9, and 205.8 nm^2/thio-SEC. The estimated surface areas for these clusters are much larger than the experimental results. The peak currents increase with the scan rate (0.01−1.0 V/s). However, the increase in peak current does not follow any regularity, for example, a linear increase with the scan rate or the square root of the scan rate, indicating the more complicated redox behavior of POMs in the SAMs.

However, the close packing of thio-SECs in their SAMs cannot explain the small electrochemical currents of POMs. Actually, the accuracy of the electrochemical method used in determining the surface coverage is highly dependent upon the structure of the monolayer film and the ability of the charge-compensating ion to access the adsorbate species that are being oxidized and reduced.[18] This method determines the electrochemical accessibility of the adsorbate, rather than surface coverage of adsorbate necessarily.[18] Therefore, given the defect-free structures of the SAMs of SEC-1, SEC-2, and SEC-3, it is not surprising that their electrochemical accessibility is substantially lower than the estimated values. Combining the above-mentioned analysis, XPS and electrochemical results, we conclude that only 8.2% for SEC-1, 9.6% for SEC-2, and 9.6% for SEC-3 moieties are being electrochemically accessed in the cyclic voltammetry experiments.[19] In contrast to the electrochemical experiments described in the literature,[18,20] the SAMs of thio-SECs are very stable in the electrochemical cycling, even in the potential windows of thio-SECs. The electrochemical experiments do not lead to increased disorder or partial desorption of the adsorbed thio-SECs, and the SAMs are still closely packed. The enhanced stability of the SAMs of thio-SECs is attributed to multiple S−Au bonds on the gold substrate (Figure 1). To test the stability of the SAMs of thio-SECs further, we exposed the SAMs to water and chloroform and then evaluated the effects using AFM. The AFM images both show an almost fully covered surface after exposure to water for 48 h or hot water at 80 °C for 1 h, which is similar to that before exposure, indicating that the SAMs are

(16) (a) Li, Y.; Bu, W.; Wu, L.; Sun, C. *Sens. Actuators B* **2005**, *107*, 921. (b) Ruhlmann, L.; Nadjo, L.; Canny, J.; Contant, R.; Thouvenot, R. *Eur. J. Inorg. Chem.* **2002**, 975.
(17) Brown, A. P.; Anson, F. C. *Anal. Chem.* **1977**, *49*, 1589.
(18) Caldwell, W. B.; Campbell, D. J.; Chen, K.; Herr, B. R.; Mirkin, C. A.; Malik, A.; Durbin, M. K.; Dutta, P.; Huang, K. G. *J. Am. Chem. Soc.* **1995**, *117*, 6071.
(19) Brown, A. P.; Anson, F. C. *Anal. Chem.* **1977**, *49*, 1589.
(20) Walczak, M. M.; Popenoe, D. D.; Deinhammer, R. S.; Lamp, B. D.; Chung, C.; Porter, M. D. *Langmuir* **1991**, *7*, 2687.

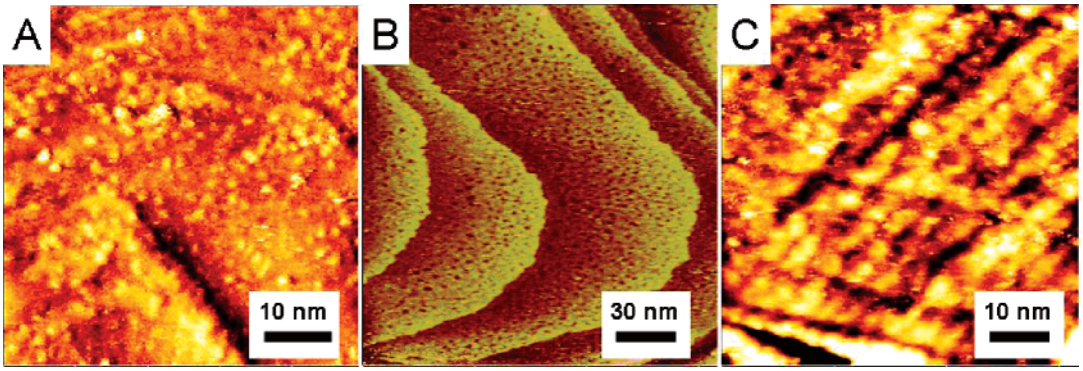

Figure 6. STM images of the SAM of SEC-3 on a gold substrate after (A) 10 min and (B) 24 h of immersion, of which C is the magnified STM image of B.

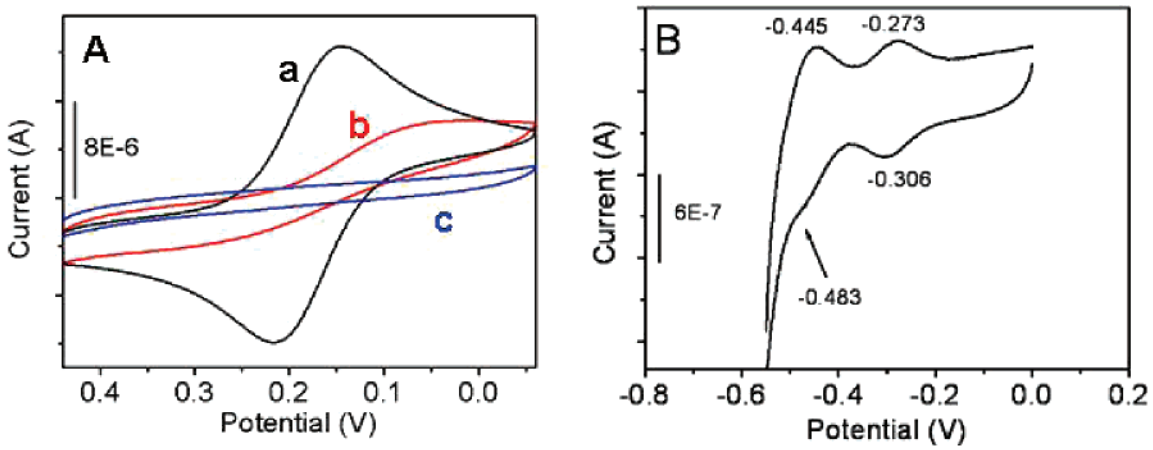

Figure 7. (A) Cyclic voltammetry for 1 mM $K_3[Fe(CN)_3]/K_4[Fe(CN)_3]$ in a 0.2 M Na_2SO_4 aqueous solution at a bare Au electrode (line a) and at the modified gold electrode of the SAM of SEC-3 after 10 min (line b) and 24 h of immersion (line c) and (B) cyclic voltammogram of a SAM of SEC-2 on a freshly polished gold electrode (supporting electrolyte, 0.2 M Na_2SO_4/0.05 M H_2SO_4 aqueous solution; scan rate, 100 mV/s).

Table 3. Electrochemical Data and Accessibility of the SAMs of SEC-1, SEC-2, and SEC-3 on Freshly Polished Gold Electrodes (Supporting Electrolyte, 0.2 M Na_2SO_4/0.05 M H_2SO_4 Aqueous Solution; Scan Rate, 100 mV/s)[a]

SAMs	E_{pa} (V)[a]	E_{pc} (V)[a]	$E_{1/2}$ (V)[a]	ΔE_p (mV)[a]	electron number	assignments	accessibility (Γ, mol/cm^2)
SEC-1	−0.280	−0.306	−0.293	26	2	W^{VI}/W^{V}	1.1×10^{-12}
	−0.428	−0.458	−0.443	30	2	W^{VI}/W^{V}	
SEC-2	−0.273	−0.306	−0.289	33	2	W^{VI}/W^{V}	1.8×10^{-12}
	−0.445	−0.483	−0.464	38	2	W^{VI}/W^{V}	
SEC-3	−0.085	−0.111	−0.098	26	2	Fe^{III}/Fe^{II}	1.5×10^{-12}
	−0.283	−0.318	−0.300	35	2	W^{VI}/W^{V}	
	−0.372	−0.399	−0.385	27	2	W^{VI}/W^{V}	

[a] E_{pa}, oxidation potential; E_{pc}, reduction potential; $E_{1/2}$, $(E_{pa} + E_{pc})/2$; ΔE_p, the difference between the pair of redox potentials.

stable in water as seen in the Supporting Information. However, the defects are evidently dispersed on the film after immersion in chloroform for 48 h, which is indicative of the partial desorption of SECs. The SAMs of SECs are stable in water presumably because of the poor solubility of SECs in water. A stable polymeric SAM was reported on the basis of multi-thiol/Au interactions.[21]

Conlusions

We have demonstrated that POM-based SAMs on gold surfaces could be prepared by using thio-SECs terminated with multiple CH_3COS- groups. Thio-SECs self-assembled into monolayers on gold sufaces through the hydrolysis of CH_3COS- groups and the subsequent formation of S−Au bounds. Furthermore, the SAMs of the thio-SECs possess closely packed structures, and the local short-range order is clearly observed in the magnified STM image. The redox of the original POMs has been well preserved in the SAMs. Compared with those reported in the literature, the SAM-modified electrodes that we obtained here are not only highly ordered with respect to local short-range order but also stable in the electrochemical cycling attributed to the multiple S−Au bonds of thio-SECs on the gold substrates, which aid in the construction of functional materials such as electrochemical and electrocatalytic devices. Here, the obtained SAM-modified electrode shows the evident catalytic reduction of residual oxygen, and further work will concentrate on the investigation of the catalytic reduction of other substrates such as hydrogen peroxide or nitrite.

Acknowledgment. We acknowledge financial support from the National Basic Research Program (2007CB808003), the

(21) Kim, T.; Chan, K. C.; Crooks, R. M. *J. Am. Chem. Soc.* **1997**, *119*, 189.

National Natural Science Foundation of China (20473032, 20731160002), PCSIRT of the Ministry of Education of China (IRT0422) and the 111 Project (B06009), and the Open Project of the State Key Laboratory of Polymer Physics and Chemistry of CAS.

Supporting Information Available: Cyclic voltammetry and AFM image of the SAM of SEC-3 on gold substrate. This material is available free of charge via the Internet at http://pubs.acs.org.

LA702335R